Study on the Influence of Water Stop Failure on Seepage Characteristics of High Concrete Face Rockfill Dam

Shengjie Di[1,*][a], Jing Liu[1] and Jiaqi Xu[2]

[1]*Northwest Engineering Corporation Limited, Power China, Xi'an, Shaanxi, 710065, China*
[2]*Hohai University, Nanjing, Jiangsu, 210098, China*

Abstract: Aiming at the problem of seepage stability of concrete face rockfill dam, this paper combines the independently developed Northwest Hydropower Earth-rock Dam Seepage Calculation Platform to carry out finite element calculation and analysis on the influence of water stop failure on seepage characteristics of dam body under different schemes. The results show that when the water stop of the panel joint is completely invalid, the parameters such as water level seepage in the dam body are significantly increased compared with the complete water stop of the panel joint. The failure water head distribution in the middle of the panel joint is close to that of the middle and high failure, indicating that the middle failure is more dangerous than the failure of the higher and lower positions of the panel joint.

1 INTRODUCTION

As a new type of earth-rock dam developed in recent decades, concrete face rockfill dam has been recognized by scholars at home and abroad because of its good safety, wide adaptability, convenient construction and local materials, and has been widely used in water conservancy and hydropower projects at home and abroad (Chen et al., 2011). According to the actual operation state of a large number of face rockfill dams that have been built, the seepage stability problem is prominent due to the panel rupture, joint opening and water stop failure caused by dam deformation and uneven settlement, which affects the normal operation of the project and even affects the dam safety or dam failure (Pan et al., 2008). This phenomenon is more obvious for high dams. Therefore, seepage stability analysis is of great significance for the long-term safe and stable operation of CFRD (Xiong et al., 2015; Lin et al., 2012; Shakya et al., 2019).

With the development of modern computing technology and the powerful computing power of computer, numerical simulation method has become one of the important methods for seepage stability analysis of concrete faced rockfill dam. In this paper, the influence of concrete panel water-stop joint failure on the seepage characteristics of dam body is studied by using the Northwest Hydropower-rock Dam Seepage Calculation Platform (NWHDSCP) developed by the author 's project team, which provides a basis for evaluating the safety and stability of dam body and structural design and optimization design.

2 BASIC THEORY OF SATURATED-UNSATURATED SEEPAGE

The basic differential equation of unsaturated seepage is derived by the same method as saturated seepage under the assumption that Darcy 's law is also applicable to unsaturated seepage. The basic differential equation of unsteady saturated-unsaturated seepage is as follows:

---

[a] https://orcid.org/0009-0003-2095-6560

$$\frac{\partial}{\partial x_i}\left[k_{ij}^s k_r(h_c)\frac{\partial h_c}{\partial x_j}+k_{i3}^s k_r(h_c)\right]-Q=\left[C(h_c+\beta S_s)\right]\frac{\partial h_c}{\partial t} \qquad (1)$$

where, h_c is pressure head. k_{ij}^s is saturated permeability coefficient tensor. k_{i3}^s is the permeability coefficient value in the saturated permeability coefficient tensor is only related to the third coordinate axis. k_r is relative water permeability. C is moisture capacity. β is Saturated-unsaturated selection constant. S_s is elastic specific storage. Q is source term.

Considering rainfall infiltration, the definite conditions of the unsteady saturated-unsaturated seepage differential equation include initial conditions and boundary conditions, which are briefly described as follows:

$$h_c(x_i,0)=h_c(x_i,t_0), \quad i=1,2,3 \qquad (2)$$

$$h_c(x_i,t)\big|_{\Gamma_1}=h_{c1}(x_i,t) \qquad (3)$$

$$-\left[k_{ij}^s k_r(h_c)\frac{\partial h_c}{\partial x_j}+k_{i3}^s k_r(h_c)\right]n_i\big|_{\Gamma_2}=q_n \qquad (4)$$

$$-\left[k_{ij}^s k_r(h_c)\frac{\partial h_c}{\partial x_j}+k_{i3}^s k_r(h_c)\right]n_i\big|_{\Gamma_3}\geq 0 \qquad (5)$$

$$-\left[k_{ij}^s k_r(h_c)\frac{\partial h_c}{\partial x_j}+k_{i3}^s k_r(h_c)\right]n_i\big|_{\Gamma_4}=q_r(t) \qquad (6)$$

where, n_i is outer normal direction cosine of boundary surface. t_0 is initial time. h_{c1} is known water head. q_n is known flow. $q_r(t)$ is rainfall infiltration flow. Γ_1 is deterministic hydraulic head boundary. Γ_2 is known flow boundary. Γ_3 is rainfall infiltration boundary. Γ_4 is saturated escape surface boundary.

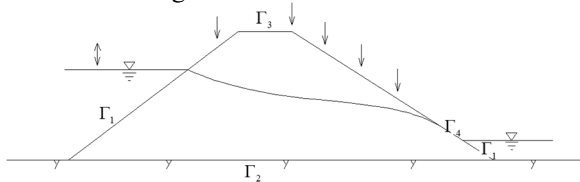Taking the earth dam as an example, the schematic diagram of the seepage boundary conditions in Figure 1.

Figure 1: The schematic diagram of seepage boundary.

3 SIMULATION PROCESS

NWHDSCP is developed based on Intel Visual Fortran, and its process includes three parts : pre-processing, calculation and post-processing. The process diagram is shown in Figure 2.

The pre-processing section includes grid file IIIN.dat, constraint file IIID.dat, material file IMAT.dat, earth-rock dam calculation preparation file FILESET.dat and seepage calculation process file ISEEP.dat. In the calculation plate, the finite element calculation principle, convergence criterion and boundary condition processing method are used to calculate and analyze the files that have been generated in the pre-processing plate. The platform has a perfect post-processing interface. The results show that the results are closely combined with the needs of engineers. In addition to the basic displacement and stress cloud diagram, it also includes parameters closely concerned in engineering such as seepage flow of different materials and settlement velocity of soil filling.
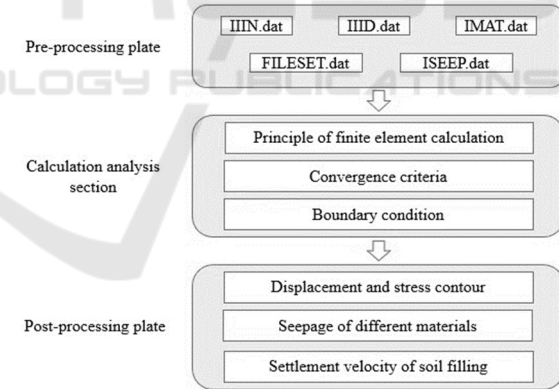

Figure 2: NWHDSCP Simulation process.

4 RESEARCH SCHEME AND ANALYSIS MODEL

4.1 Research Scheme

The project is a concrete face rockfill dam. The elevation of the foundation surface is 3711.50 m, the elevation of the dam crest is 3900.50 m, the width of the dam crest is 10.0 m, the total length of the dam

crest is 510.0 m, and the maximum dam height is 189.0 m. The slope ratio of the upstream dam slope is 1:1.4, and the cover weight area and the upstream cover area are set at the elevation of 3797.00 m. The slope ratio of the downstream dam slope is 1: 1.5 above the elevation of 3848.50 m, and 1:1.4 below the elevation of 3848.5. The calculation condition adopts the normal storage level condition, the upstream water level is 3892.00 m, and the downstream water level is 3721.81 m. The dam body partition and typical section diagram are shown in Figure 3. The research scheme are as flollws.

Scheme 1(S-1): The waterstop system is in good condition.

Scheme 2(S-2): All panel joints fail.

Scheme 3(S-3): The local failure of the panel joint is 5m long, which is located at the dam height of 5m, 100m and 180m.

Scheme 4(S-4): The local failure of the panel joint is 5 m long, which is located at 180 m high of the dam.

Scheme 5(S-5): The local failure of the panel joint is 5 m long, which is located at 100 m high of the dam.

Scheme 6(S-6): The local failure of the panel joint is 5 m long, which is located at 5 m high of the dam.
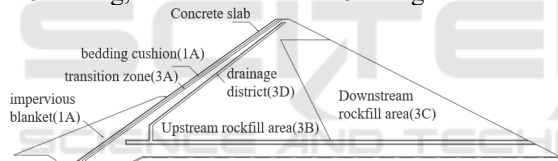

Figure 3: Computed profile diagram.

4.2 Analyze the Model and Parameters

The typical calculation section diagram of the upper section is simplified, and the three-dimensional model is established and meshed by NWHDSCP.A total of 5 panels (single width 12m) are established. The length of the model is 2307m, of which the length above the dam axis is 1152m, and the dam axis is 1155m below the dam axis. The bottom elevation of the model is taken to 2918.5m elevation, and the depth of the intercepted dam foundation is about 4 times the maximum dam height, which meets the requirements of finite element calculation. The model is divided into 488900 mesh elements and 518271 nodes. The three-dimensional model and grid diagram are shown in Figure 4 and Table 1.
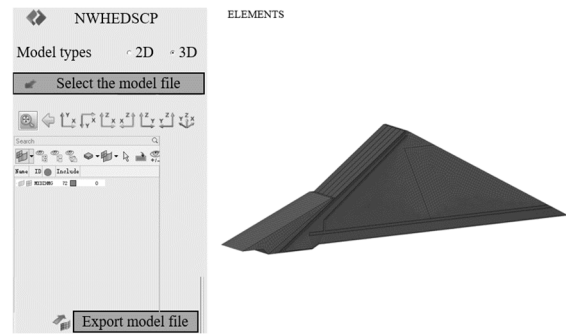

Figure 4: Finite element analysis model.

Table 1: permeability coefficient of each material area.

Material	Permeability coefficient （cm/s）	Allowable hydraulic slope of landside
Concrete slab	1.00×10^{-7}	200.00
Bedding cushion (2A)	5.83×10^{-4}	0.25
Transition zone (3A)	5.39×10^{-4}	0.20
Upstream rockfill area (3B)	2.14×10^{-2}	\
Downstream rockfill area (3C)	2.07×10^{-3}	\
Impervious blanket (1A)	1.00×10^{-5}	\
Drainage district (3D)	5.00×10^{-1}	\

4.3 Hydraulic Gradient of Each Material Partition

According to the flow velocity value of each material partition, the maximum hydraulic gradient of each calculation scheme is calculated, and the analysis results are shown in Table 2. It can be seen from the table that when the local water stop failure occurs in the face joint, the cushion and the transition material play a certain role in retaining water, and the maximum hydraulic gradient value increases significantly. The maximum gradient of the cushion and the transition material is 3.8 and 0.8; when all the water-stop joints fail, the anti-seepage ability of the cushion and the transition material is insufficient, the water level line inside the dam body rises obviously, the maximum hydraulic gradient value is greater than the local failure, and the maximum gradient of the cushion and the transition material is 14.86 and 2.27.

Table 2: Permeability coefficient of each material area.

Scheme	Concrete slab	2A	3A	3B	3C	3D
S-1	150.60	0.03	0.02	0.04	/	0.07
S-2	34.20	14.86	2.27	0.05	0.18	0.09
S-3	146.80	3.81	0.81	0.04	/	0.52
S-4	150.60	0.03	0.03	0.04	/	0.10
S-5	149.10	2.93	0.65	0.04	/	0.42
S-6	149.40	0.03	0.03	0.04	/	0.11

Table 3: Permeability coefficient of each material area.

Scheme	Concrete slab	Impervious curtain	Bed rock	Total
S-1	0.5	12.5	2.9	15.9
S-2	1548.0	11.7	2.8	1562.5
S-3	323.1	10.4	2.6	336.1
S-4	104.3	12.5	2.9	119.7
S-5	317.3	10.4	2.6	330.3
S-6	10.2	12.5	2.9	25.6

4.4 Seepage Flow in Each Partition

The calculation section of seepage flow is divided into three sections : dam body, anti-seepage curtain and bedrock. The seepage flow of each partition under each calculation scheme of concrete face rockfill dam is shown in Table 3. It can be seen from the table that when all the panel joints fail, the seepage flow through the dam increases sharply, and is significantly higher than the local failure. When the water stop at the bottom of the panel joint fails, the seepage flow through the dam body is significantly lower than that in the middle and high parts. The main reason is that the cover and cover weight on the upstream side of the dam body play a certain anti-seepage role, and the water stop failure of the panel joint has little effect on the seepage flow of the anti-seepage curtain and bedrock in Figure 5.

4.5 Analysis of Dam Head

When the panel joint is used normally, the water head in the dam body is significantly reduced, and the anti-seepage effect of the panel is obvious. When all the panel joints fail, the water head in the dam body is large and decreases slowly along the flow direction; when the height of the panel joint fails, the water head is dense near the failure position, and the water head in the dam body is higher in the upstream rockfill area, but it decreases rapidly along the flow direction. The distribution of failure water head in the middle of the panel joint is close to that of the middle and high failure, which indicates that the middle failure is more dangerous than the higher position of the panel joint and the lower position of the upstream blanketing effect. When the water stop at the bottom of the panel joint fails, it has little effect on the water head in the dam body.
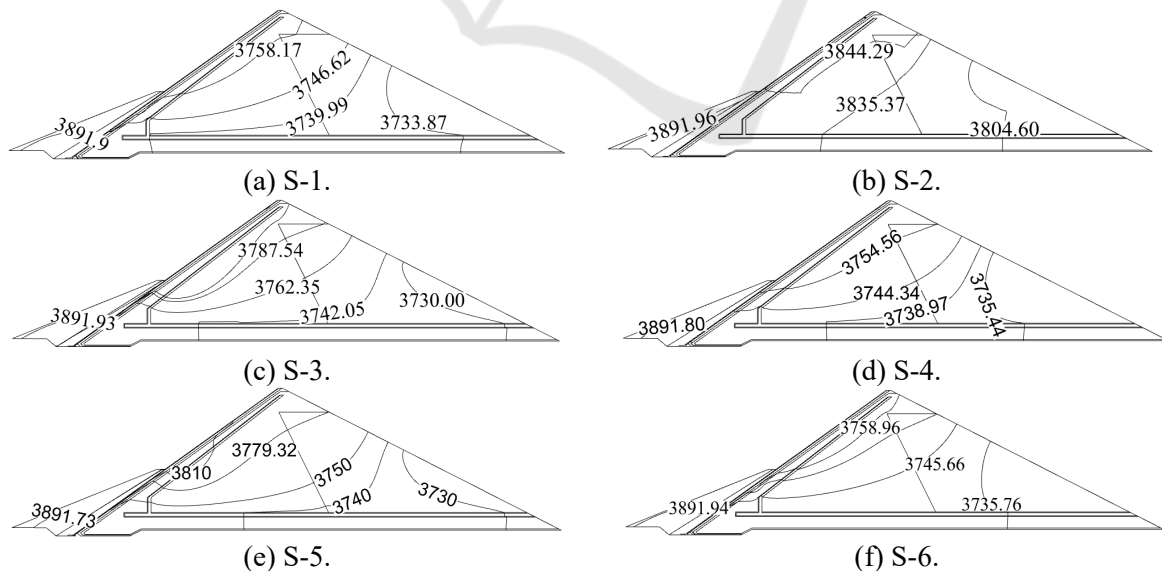

(a) S-1.

(b) S-2.

(c) S-3.

(d) S-4.

(e) S-5.

(f) S-6.

Figure 5: Equal water head isoline map.

5 CONCLUSION

When all the water stops of the panel joints fail, the water level line in the dam body rises obviously, which is much higher than the action range of the drainage body. There is also a saturated zone in the downstream rockfill area, and the seepage flow through the dam body increases sharply. The maximum slope of the cushion and the transition material reaches 14.86 and 2.27.

When the height and height of the face slab joint fail, the water level in the dam body increases significantly in the upstream rockfill area, but soon decreases to the range of the drainage body, and the maximum slope of the cushion and transition material is 3.8 and 0.8 ; the distribution of failure water head in the middle of the panel joint is close to that of the middle and high failure, indicating that the middle failure phase is more dangerous than the higher position of the panel joint and the lower position of the upstream blanketing effect.

ACKNOWLEDGMENTS

REFERENCES

Chen, S.K, Yan, J, Li, J.M., 2011. Seepage field 3D finite element simulation of concrete faced rockfill dam under failure condition of vertical fracture. *Rock and Soil Mechanics*, (11): 3473-3478.

Pan, S.H, Mao, X.Y., 2008. Seepage field finite element simulation of faced rockfill dam under cases of vertical joints and seal failure. *Rock and Soil Mechanics*, 29(S1): 145-148.

Xiong, L, Dang, F.N, Zhang, H.F., 2015. Seepage field analysis of a concrete face rockfill dam after water stop failure. *Water Resources and Power*, 33(06): 80-83.

Lin, Q.M, Gong, J., 2012. Analysis of influence of panel cracking on seepage characteristics of concrete face rockfill dam. *Jilin Water Resources*, (10): 1-4.

Shakya, C, Luo, X.Q., 2019. Coupling Internal Erosion through Concrete Face Rockfill Dams with Damage in Face Slab under Impounding. *Journal of Physics: Conference Series*, 1176(5): 052067(13app).